

1 High-resolution quantification of the rhizosphere effect 2 along a soil-to-root gradient shows selection-driven 3 convergence of rhizosphere microbiomes

4
5 Sanne W.M. Poppeliers^a, Juan José Sánchez-Gil^a, José Luis López^{b,c,d}, Bas E. Dutilh^{b,d}, Corné M. J.
6 Pieterse^a and Ronnie de Jonge^{a,e,*}

7
8 ^aPlant-Microbe Interactions, Department of Biology, Science for Life, Utrecht University, 3584CH, Utrecht,
9 The Netherlands

10 ^bTheoretical Biology and Bioinformatics, Department of Biology, Science for Life, Utrecht University, 3584CH,
11 Utrecht, The Netherlands

12 ^cInstituto Andino Patagónico de Tecnologías Biológicas y Geoambientales, Bariloche, Rio Negro, Argentina

13 ^dInstitute of Biodiversity, Faculty of Biological Sciences, Cluster of Excellence Balance of the Microverse,
14 Friedrich-Schiller-University Jena, 07743, Germany

15 ^eAI Technology for Life, Department of Computing and Information Sciences, Department of Biology, Utrecht
16 University

17
18 *Correspondence: r.dejonge@uu.nl

19 **Abstract**

20
21 Plants secrete a complex array of organic compounds, constituting about a third of their photosynthetic
22 products, into the surrounding soil. As a result, concentration gradients are established from the roots into the
23 bulk soil, known as the rhizosphere. Soil microbes benefit from these root exudates for their survival and
24 propagation, and consequently, the composition of the rhizosphere microbial community follows the gradient
25 of available compounds, a phenomenon oftentimes referred to as the rhizosphere effect. However, the fine-
26 grained changes in the microbial community along this soil-root gradient have not been well described. Yet
27 such insights would enable us to underpin the ecological rules underlying root microbial community assembly.
28 Therefore, here we harvested the roots of individual *Arabidopsis thaliana* plants grown in three different natural
29 soils at high-resolution, such that we could interrogate community assembly and predict microbial growth rate
30 across consecutive, fine-grained, rhizosphere 'compartments'. We found that the strength of the rhizosphere
31 effect depends on root proximity and that microbial communities closer to the roots harbour related microbes.
32 Closer to the roots, microbial community assembly became less random and more driven by selection-based
33 processes. Intriguingly, we observed priority effects, where related microbes that arrive first are more likely to
34 establish, and that microbes might use different ecological growth strategies to colonise the rhizosphere. All
35 effects appeared to be independent from starting conditions as microbial community composition converged
36 on the root despite different soil 'microbial seed banks'. Together, our results provide a high-resolution view
37 of the microbiome changes across the soil-root gradient.

38

39 **Key words**

40 Plant root microbiome, rhizosphere effect, soil-root gradient, priority effects, natural selection

41

42 Introduction

43
44 As molecules diffuse through a matrix, they dilute as they move further away from the source. The same
45 principle holds for plant roots and their exudates. Plants secrete a complex array of organic compounds into
46 the soil¹, about a third of their photosynthetic products². As a result, concentration gradients are established
47 from the roots into the bulk soil and vice versa³. For example, in ryegrass, the concentration of soluble organic
48 carbon compounds including soluble sugars and oxalic acid decreased further away from the roots⁴. The soil
49 surrounding the roots that is influenced by root activity is called the rhizosphere⁵. Its shape and size depend on
50 plant properties and soil type⁶. The rhizosphere is both dynamic and gradual, as roots continue to grow and
51 explore new parts of the surrounding soil and microhabitat properties gradually change from root to bulk soil³.
52

53 Because the rhizosphere is a carbon-rich environment, it is a hotspot for microbial activity^{7,8}. Rhizosphere
54 microbial communities are often different from the surrounding bulk soil, a pattern that is referred to as the
55 ‘rhizosphere effect’^{9–13}. The root-associated microbiome has a higher cell density^{15,16}, is often less diverse, and
56 harbours a distinct set of species^{14,15}. Since soil microbes are (partly) dependent on root exudates for their
57 survival, rhizosphere microbial community composition most likely follows the gradient of available
58 metabolites, gasses, ions, and other substances^{3,16}. Many, diverse rhizosphere-competent taxa that contribute
59 to the separation between bulk soil and rhizosphere microbial communities have been identified¹⁷, yet how
60 microbial community composition differs on smaller scales along the soil-root gradient is still largely unknown.
61

62 The rhizosphere effect in *Arabidopsis thaliana* (hereafter Arabidopsis), an extensively studied model plant, is
63 often found to be relatively small^{18–21}, especially compared to plant species with a longer life history²² or crops
64 like wheat, oat, and pea²¹. In these studies, the rhizosphere is defined as ‘loosely adhering soil’²³. However,
65 evidence points out that for microbial communities firmly attached to the root (often referred to as the
66 ‘rhizoplane’), the rhizosphere effect in Arabidopsis is comparably strong²². It is likely that the observed
67 rhizosphere effect not only depends on the amount and composition of root exudates and their diffusion rates
68 through the soil, but also on how the rhizosphere is collected. For Arabidopsis, which has relatively small roots
69 compared to large crops such as maize and wheat, different sampling strategies might be necessary to reveal
70 the scope of the root influence, in order to fully explore how rhizosphere microbial communities are assembled,
71 and assess what taxa and functions are associated with rhizosphere competence.
72

73 To better understand establishment of the rhizosphere microbial community, it is essential to characterize
74 processes underlying its assembly. Traditionally, microbial community assembly is most often explained by
75 mechanisms of selection²⁴, while more and more studies show that in complex communities, chance, and

76 environmental heterogeneity can be equally important^{25–28}, also in the rhizosphere^{29,30}. This might be especially
77 relevant when trying to engineer plant microbiomes using plant-beneficial microbes³¹. Given that the root
78 microbiome is mainly formed by a variety of microbes present in the surrounding bulk soil³², as well as those
79 originating from seeds or carried by the air^{33–35}, it is probable that random processes have a greater impact in
80 the rhizosphere than, for instance, the mammalian gut, where numerous microbes are transmitted during
81 birth³⁶. Who ends up in the rhizosphere is primarily driven by the resident soil microbial community, and who
82 can colonize first³⁷, and only secondarily through selection by the plant, depending on root proximity. While
83 there is a substantial amount of research on taxa, genes or traits that are enriched in the rhizosphere under
84 specific circumstances, it is still not clear what ecological community assembly processes steer this
85 environment³⁸.

86

87 With this study we wanted to determine the strength and dynamics of the rhizosphere effect in *Arabidopsis*
88 across the soil-root continuum, characterize the changes in microbial community composition along this
89 gradient and assess the importance of selective and random community assembly processes. To do so, we grew
90 *Arabidopsis* plants in natural soil sampled from the same geographic location over three different years and
91 harvested the rhizosphere in a reproducible manner such that the microbiome in each consecutive
92 ‘compartment’ could be measured and compared to the microbes in the unplanted bulk soil. We focused on
93 the bacterial portion of the rhizosphere microbiome, the largest microbial portion³⁹, and found that the strength
94 of the rhizosphere effect in *Arabidopsis* is dependent on root proximity. Bacterial communities closer to the
95 roots harbour phylogenetically similar microbes, even though different microbes are detected across samples,
96 a phenomenon that we attribute to the influence of priority effects. As we sampled closer to the roots, we
97 found that microbial community assembly became less random and was more driven by selection-based
98 processes, and this effect was largely independent from starting conditions as microbial communities converged
99 on the root despite different bulk soil ‘microbial seed banks’.

100

101 Materials and Methods

102

103 Soil collection and preservation

104

105 The soil used in this study was taken from the Reijerscamp nature reserve, the Netherlands ($52^{\circ}01'02.55''$,
106 $5^{\circ}77'99.83''$), where previously an abundant endemic *Arabidopsis* population was found⁷³. Agricultural practices
107 ended in 2000, and subsequently the area was restored as natural grassland. The soil was described by Berendsen
108 et al. 2018⁷³ as a gleyic placic podzol, consisting of coarse sand and gravel covered by a 30–50 cm top layer.
109 The top 20 cm of soil was collected in October 2018 for experiment 1 (hereafter exp 1), April 2019 for
110 experiment 2 (exp 2) and December 2019 for experiment 3 (exp 3), air dried and sieved (1 cm sieve) to remove
111 plant debris and rocks, and subsequently stored at room temperature. Prior to the experiment the soil was
mixed with 100 mL of tap water per kg of dried soil.

112

113 Experimental set-up

114

115 *Arabidopsis thaliana* accession Col-0 seeds (N1093; Nottingham *Arabidopsis* Stock Centre) were surface
116 sterilized by fumigation using a mixture of 100 mL bleach and 3.2 mL 37% HCl for 4 h. Seeds were sown on
117 1% Murashige and Skoog (MS) medium⁷⁴ with 0.5% sucrose, and after 2 days of stratification in the dark at 4
118 °C, the seeds were transferred to a growth chamber (21 °C, 70% relative humidity, 10 h light/14 h dark, light
119 intensity $100 \mu\text{mol} \cdot \text{m}^{-2} \cdot \text{s}^{-1}$) to allow germination. Two-week-old seedlings were transferred to individual 60-
120 mL pots with approximately 100 g of Reijerscamp soil. Bulk soil pots were left unplanted. Pots were watered
121 for 3 weeks every other day and during the whole experiment developing seedlings from plant seeds that came
with the soil were removed with tweezers upon detection.

122

123 Five-week-old *Arabidopsis* roots were harvested using a standardized sampling method (**Supplementary**
124 **Figure 1a**), resulting in four compartments of the soil-root gradient, in which in each consecutive compartment
125 microbiome samples were harvested in increasingly closer proximity to the root (**Supplementary Figure 1b**).
126 Exp1 was a pilot where each sample consisted of two plants, while in exp2 and exp3 we used one plant per
127 sample, and more replicates were added to accommodate in-depth analyses. For rhizosphere-4 samples (RS4),
128 roots were taken out of the soil and shaken briefly until most loose soil fell off and stored in a 2-mL Eppendorf
129 tube. For rhizosphere-3 samples (RS3) this was done similarly, and additionally roots were stripped of as much
130 soil as possible with clean gloves and by tapping the roots on clean paper before transferring them to a 2-mL
131 Eppendorf tube. For rhizoplane-2 samples (RP2), roots that were harvested the same as for the RS3 samples,
132 were transferred to a Falcon tube containing 25 mL MgSO₄ and inverted 5 times by hand. Roots were then
133 taken out, carefully dried with paper, and put in a clean 2-mL Eppendorf tube. For rhizoplane-1 samples (RP1),
134 roots were harvested according to the RS3 samples, and transferred to a Falcon tube containing 25 mL

135 phosphate-Silwet (PBS-S) buffer (per L 6.33 g NaH₂PO₄.H₂O, 10.96 g Na₂HPO₄.2H₂O and 200 µL Silwet L-
136 77) and vortexed on maximum speed for 15 s. After this, the roots were transferred to a new Falcon tube with
137 25 mL PBS-s buffer and vortexed again for 15 s. Roots were then taken out, dried with paper, and transferred
138 to a clean 2-mL Eppendorf tube. Up to 0.25 g of bulk soil was taken from each unplanted pot. Root or soil
139 samples were flash frozen in liquid N₂ directly after sampling and stored at -80 °C.

140

141 DNA isolation and 16S amplicon sequencing

142 DNA extractions for exp1 and exp2 were done with the Mo Bio PowerSoil kit (Qiagen, Germantown, USA)
143 according to the manufacturer's instructions with one adjustment optimized for Reijerscamp soil: after addition
144 of lysis buffer and solution C1, samples were additionally incubated at 70 °C for 10 min. The remaining steps
145 were performed as described by the manufacturer's instructions. For exp3, DNA extractions were performed
146 with the MagAttract PowerSoil DNA kit (Qiagen, Cat. No. 27000-4-KF) optimized for the KingFisher™ Flex
147 Purification System (Thermo Scientific, 183 Waltham, MA, USA). DNA quality and quantity was checked using
148 a NanoDrop 1000 spectrophotometer (Thermo Scientific, 183 Waltham, MA, USA). For exp 1, we pooled
149 DNA of two individual samples from the same compartment. All sampled were normalized to 5 ng · µL⁻¹.
150 Subsequently, we amplified the hypervariable V3-V4 region of the 16S rRNA gene with phasing primers
151 CCTACGGGNNGGCWGCAG and GACTACHVGGGTATCTAATCC (**Supplementary Table 3**), using the
152 standard protocol from Illumina. In short, the amplification reaction mixture contained 2.5 µL of sample, 5 µL
153 of primer mix, 5 µL PCR grade water and 12.5 µL KAPA HiFi HotStart ReadyMix (Roche, Indianapolis, USA).
154 The PCR conditions were 98 °C for 5 min, 25 cycles of 98 °C for 40 s, 55 °C for 30 s, 72 °C for 60 s and a final
155 extension at 72 °C for 10 min. For the index PCR the reaction mixture contained 2.5 µL of DNA from PCR 1,
156 2.5 µL of each primer, 5 µL PCR grade water and 12.5 µL KAPA HiFi HotStart ReadyMix (Roche, Indianapolis,
157 USA). Samples were normalized and pooled in equimolar amounts and the pools were sequenced on the
158 Illumina MiSeq machine with the 2 x 300 bp V3 kit at the USEQ sequencing facility (Utrecht University, the
159 Netherlands).

160

161 Bioinformatics and statistical analysis

162 Raw sequencing data was processed with Qiime2 version 2019.7⁷⁵. Each individual sequencing run (1 for exp
163 1, 2 for exp 2 and exp 3) was processed separately as follows. After importing the data, primers were removed
164 using *Cutadapt* 2.8⁷⁶. Raw sequence data were demultiplexed and quality filtered using the q2-demux plugin
165 followed by denoising with DADA2⁷⁷ (via q2-dada2) where sequences were clustered into Amplicon Sequence
166 Variants (ASVs) at >99% identity. Singletons and doubletons were removed, and data from individual
167 sequencing runs was merged. Taxonomy was assigned to the ASVs based on the SILVA reference database
168 (99% similarity version 132) using the classify-consensus-vsearch plugin (VSEARCH 2022.8.0)^{78,79}. After pre-

169 processing of the sequencing data, $\sim 2.23 \cdot 10^7$ reads remained and were clustered into 35762 ASVs from three
170 experiments and 225 samples. Mean number of reads per sample was 99,092 reads, and 8 samples per
171 compartment for exp1, and 18 samples per compartment for exp2 and exp3 were retained. All subsequent
172 analyses were executed in R Statistical Software (v4.1.3; R Core Team 2022). The package *Phyloseq*⁸⁰ was used
173 to obtain the number of plant reads, read depth, and α - and β -diversity, where plant reads (chloroplasts and
174 mitochondria) were removed before analysis. From the top 50 ASVs that most strongly influence the
175 ordination, we calculated their association with PC1 as $\text{abs}(\text{PC2})$. The Sloan neutral model for prokaryotes²⁵
176 was implemented on a rarefied feature table (10,000 reads per sample), using an adjusted publicly available
177 script by Burns and co-authors (2016)²⁶. For estimation of abundance-weighted growth rate potential we largely
178 followed Lopez et al. 2023³⁷. In short, we first extracted genus-level estimates from the EGGO database⁸¹
179 which includes predicted minimum doubling times (PMDTs) for over 217,000 prokaryotic genomes and
180 computed the median PMDT for each genus. Next, we summed the abundances of each ASV within a genus,
181 and computed abundance-weighted growth rate potential for each sample type by multiplying the relative
182 abundance of each genus with the genus-specific PMDT and taking the median of those values as representative
183 for a specific compartment.

184

185 Data availability

186 The raw 16S rRNA amplicon sequencing data generated and used in this study have been deposited at the
187 NCBI Sequence Read Archive (BioProject: PRJNA1117364) and are publicly available as of the date of
188 publication.

189

190 Results

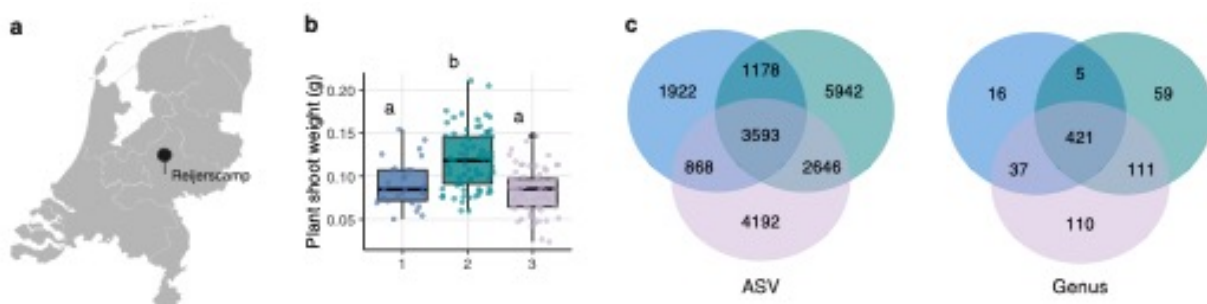
191

192 Similar plant phenotypes and starting microbiomes with different soil batches

193 To study the rhizosphere effect in *Arabidopsis* along a soil-root gradient, we conducted three experiments in
194 which we sampled roots in similar ways. We assessed the reproducibility of the rhizosphere assembly process
195 by using three comparable soil batches obtained from the same natural site over multiple years (the Reijerscamp
196 nature reserve, 52°01'02.55", 5°77'99.83"; **Figure 1a**). Soil batches were harvested in different seasons: for
197 experiment 1 (exp1) and experiment 3 (exp3) material was collected in the fall (October 2018 and December
198 2019 respectively) and for experiment 2 (exp2) this was during spring (April 2019). To evaluate whether the
199 different soil batches affect plant performance, - this could influence our ability to assess rhizosphere
200 microbiome assembly reproducibility -, we measured plant biomass in each experiment. We note that plants
201 grown on all batches displayed similar growth with only limited variation between experiments. Shoot weight

202 was ~1.5 times higher in exp2 than in exp1 and exp3 which had similar shoot weights (**Figure 1b**; ANOVA,
203 $p<0.05$).

204
205 For each experiment, we systematically collected the root-soil interphase in five high-resolution ‘compartments’
206 along the soil-root gradient: soil (S), rhizosphere-4 (RS4), rhizosphere-3 (RS3), rhizoplane-2 (RP2) and
207 rhizoplane-1 (RP1) (**Supplementary Figure 1**, see Materials and Methods), and profiled the bacterial
208 communities by amplicon-based sequencing targeting the V3-V4 region of the *16S rRNA* gene. To evaluate
209 whether the different soil batches have comparable microbial communities, we first evaluated the overlap in
210 amplicon-sequence variants (ASVs) and genera in these soils. Of all ASVs, 40% was found in ≥ 2 experiments,
211 while 75% of all genera in our dataset occurred in ≥ 2 experiments (**Figure 1c**). The ASVs identified in the soil
212 samples of the different experiments were mostly unique, but phylogenetically similar due to a high overlap at
213 the genus level, thus indicating comparable microbial starting conditions across all three experiments.
214



215
216 **Figure 1 Similar plant phenotypes and starting microbiomes between different soil batches.** **a** Sampling location of the
217 Reijerscamp nature reserve in the Netherlands. **b** Plant shoot weight per experiment. Plants from exp2 had ~1.5x higher shoot weight
218 than plants from exp1 and exp3. **c** Overlap in number of ASVs (left) and genera (right) per experiment. For ASVs, 40% was found in
219 ≥ 2 experiments, while 75% of all genera in our dataset occurred in ≥ 2 experiments.

220
221 Strength of rhizosphere effect gradually increases towards the root

222 With comparable microbial starting conditions established, our focus shifted to a more detailed examination of
223 the soil-root continuum. Moving progressively from RS4-RP1, we sampled roots with less adhering soil as
224 sample weight decreased significantly between consecutive compartments for exp2 and exp3 and was on
225 average 4.7 ± 0.9 times lower in RP1 compared to S (**Figure 2a**). Consequently, the microbial community was
226 expected to be increasingly influenced by the plant when sampling from RS4 to RS1. Because these consecutive
227 compartments include the plant root itself (**Supplementary Figure 1**, see Materials and Methods), we could
228 use the amount of plant reads in our samples as a proxy for root distance. The percentage of plant reads
229 (assigned taxonomy either ‘chloroplast’ or ‘mitochondria’) in our samples gradually increased when sampling
230 closer to the roots ($S < RS4 < RS3 < RP2 < RP1$; $0.157 \pm 0.215\%$ in S to $37.0 \pm 14.4\%$ in RP1) providing a data-
231 driven way to quantify the distance to the roots (**Figure 2b, Supplementary Table 1**; Kruskal-Wallis,
232 $p<0.001$).

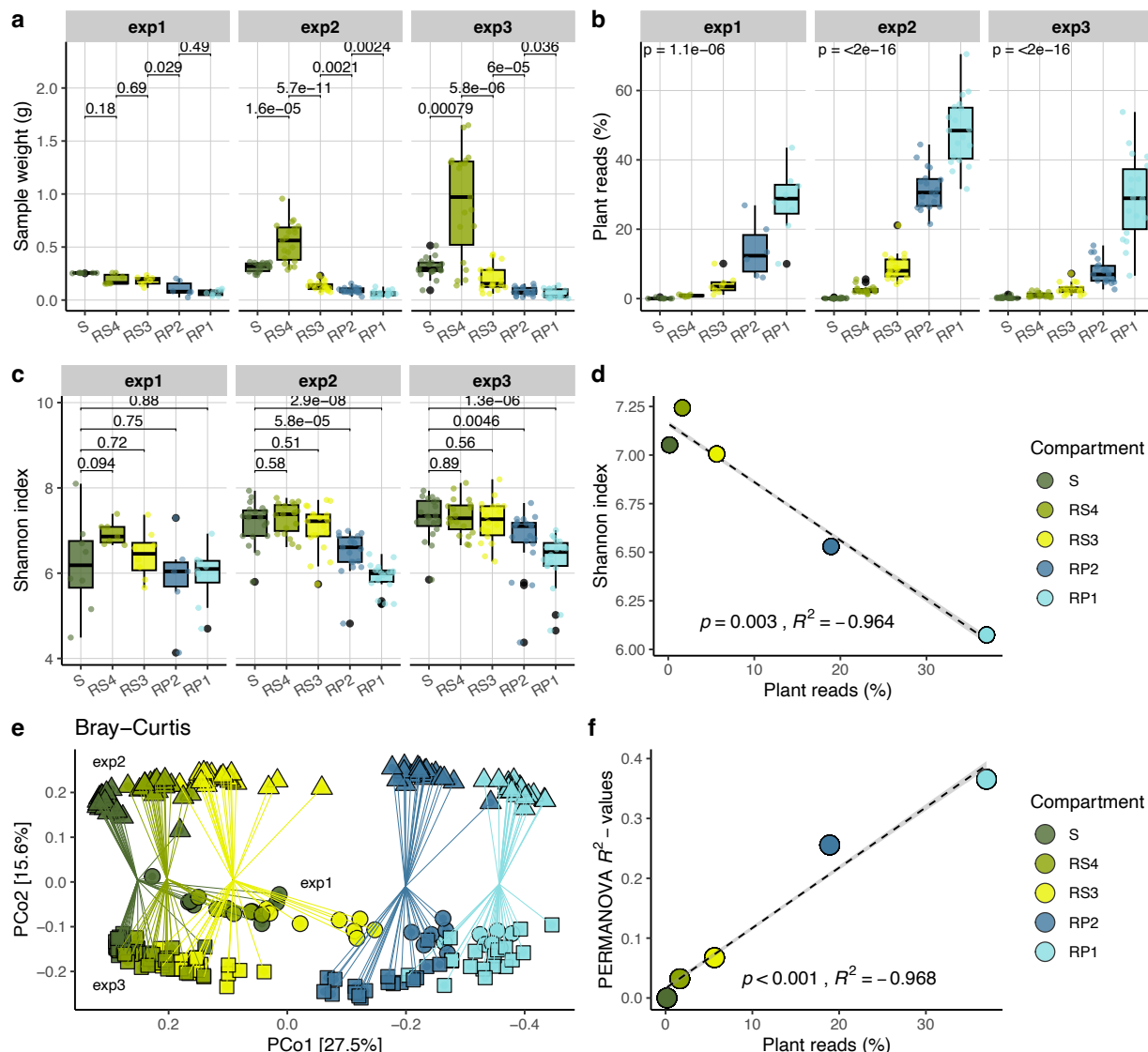
233

234 Using the microbiome datasets sampled along the soil-root gradient, we then tested whether the alpha diversity
235 (hereafter α -diversity) within our microbial communities decreased from bulk soil to rhizosphere and rhizoplane
236 by calculating and comparing the Shannon index. The Shannon index is mostly driven by evenness⁴⁰ and is
237 more robust to inherently noisy *16S rRNA* ASV data⁴¹. In exp2 and exp3, the α -diversity decreased relative to
238 S for the rhizoplane (RP2 and RP1), with the lowest values for the RP1 samples (**Figure 2c**; Wilcoxon test, p
239 < 0.05). α -diversity, which can be seen as a measure for the strength of the rhizosphere effect, correlates linearly
240 with the percentage of plant reads, i.e. with the distance to the roots (**Figure 2d**; Spearman, p = 0.003, R^2 = -
241 0.982).

242

243 To compare the microbial community composition along the soil-root gradient between experiments, we
244 measured between-sample beta-diversity (hereafter β -diversity) between all pairs of samples using the Bray-
245 Curtis dissimilarity measure and used these as input for a Principal Coordinate Analysis (PCoA) to visualize the
246 differences. We then plotted the samples from all five compartments along the first two principal coordinates
247 (PCos) of the PCoA. The distance to the plant root was the main factor that separated the samples along PCo1,
248 which explained 27.5% of the variation in the dataset (**Figure 2e**). Differences between the three experiments
249 with different soil batches represented the second most important factor along PCo2 (15.6% explained
250 variation), and exp1 and exp3 were more similar to each other than exp2. Exp1 and exp3 were performed with
251 soil batches collected from the same season (fall), while the soil from exp2 was collected in spring which might
252 explain these observations. The results of pairwise permutational multivariate analysis of variance
253 (PERMANOVA) using 999 permutations showed that there is a clear difference in the microbial community
254 composition for each compartment-experiment combination (Adonis, p = 0.001). Although the rhizosphere
255 effect is significant for RS4 samples which are most similar to S as they contain most soil, the effect size is small
256 (R^2 = 0.027). The microbiome of the RS3, RP2 and RP1 samples progressively differed from S (R^2 = 0.063,
257 0.26 and 0.37). Similar as for α -diversity, the R^2 -values that represent the strength of the rhizosphere effect
258 correlate very well with the percentage of plant reads (Pearson, p < 0.001, R^2 = 0.984; **Figure 2f**). In conclusion,
259 our sampling strategy effectively captures various high-resolution zones along the soil-root gradient and
260 reinforces that the rhizosphere effect, wherein root activity influences the microbiome, strengthens gradually
261 towards the root.

262



263

264 **Figure 2 Stronger rhizosphere effect closer to the root.** **a** Sample weight in grams for each compartment in each experiment.
265 Numbers indicate p-values with Bonferroni-correction for multiple testing (Wilcoxon test). **b** Percentage of plant reads in each
266 compartment (Kruskal-Wallis, $p < 0.001$, **Supplementary Table 1**). **c** Shannon index for each compartment in each experiment
267 depicting the microbial diversity per sample. This index integrates both species evenness and species richness. **d** Strength of the
268 rhizosphere effect quantified by the reduction in microbial diversity (Shannon index) closer to the root. The percentage of plant reads
269 is used as a proxy for sample-root distance. **e** Principal coordinate analysis (PCoA) plot based on Bray-Curtis dissimilarity highlighting
270 reproducibility of the soil-root gradient sampling (PCo1) across multiple experiments (PCo2). **f** The pairwise PERMANOVA R^2 -values
271 of the compartment community composition difference compared to soil are used as an indicator of the strength of the rhizosphere
272 effect (Pearson; $p < 0.001$, $R^2 = 0.984$). Compartments are indicated by abbreviations: soil (S), rhizosphere-4 (RS4), rhizosphere-3 (RS3),
273 rhizoplane-2 (RP2) and rhizoplane-1 (RP1).

274

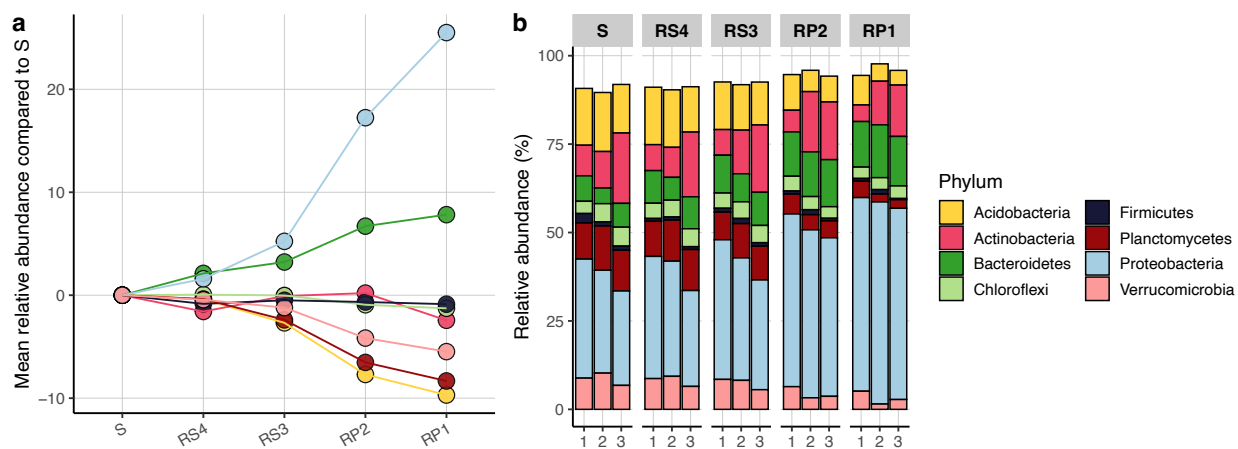
275 Proteobacteria and Bacteroidetes replace other phyla on the roots

276 Our results show that the community composition of the compartments increasingly changes along the soil-
277 root gradient, and that rhizoplane (RP2 and RP1) compartments have significantly lower diversity than soil
278 samples. To explore what taxa are mainly causing this decrease in diversity we calculated the relative abundance

279 of the major phyla that were present in all experiments (more than 5% relative abundance in a compartment
280 within an experiment, **Figure 3**^a). In line with previous studies^{18,19,22},
281 *Proteobacteria* were on average the most abundant phylum across all experiments ($39.0 \pm 11.2\%$) and their relative
282 abundance was 1.9 times higher in RP1 compared to S (Wilcoxon test, $p < 0.001$). This was mainly due to
283 expansion of the families *Burkholderiaceae* and *Oxalobacteraceae*, which together made up $\sim 21.0 \pm 4.5\%$ and
284 $\sim 15.2 \pm 7.3\%$ of all *Proteobacteria* in RP1, respectively (**Supplementary Figure 2**). Although *Bacteroidetes* were
285 not the most abundant phylum ($9.96 \pm 3.95\%$), they showed the largest increase in relative abundance: 2.3 times
286 higher in RP1 relative to S (**Figure 3b**; Wilcoxon test, $p < 0.001$). The largest increase on the root was due to
287 the family of *Sphingobacteriaceae*, which became 9.3 times more abundant in RP1 compared to S.
288

289 Several taxa decreased in relative abundance towards the root, including *Acidobacteria*, *Planctomycetes* and
290 *Verrucomicrobia*. These phyla had comparable abundances in soil ($15.4 \pm 2.1\%$, $11.7 \pm 2.1\%$ and $8.6 \pm 2.0\%$,
291 respectively) which decreased towards the root in a similar way, resulting in their abundance being ~ 3 times
292 lower in ‘rhizoplane’ samples ($5.2 \pm 2.2\%$, $2.7 \pm 1.7\%$ and $2.7 \pm 1.4\%$, respectively; Wilcoxon test, $p < 0.001$).
293 Possibly, *Acidobacteria*, *Planctomycetes*, and *Verrucomicrobia* exhibit similar life strategies that are adapted to soil
294 specifically and therefore they could be particularly susceptible to competition from rhizosphere-competent
295 taxa. The relative abundance of *Actinobacteria*, *Firmicutes* and *Chloroflexi* varied less between compartments and
296 stayed relatively constant along the soil-root gradient. Thus, it appears that *Proteobacteria* and *Bacteroidetes* replace,
297 specifically, *Acidobacteria*, *Planctomycetes* and *Verrucomicrobia* closer to the roots.
298

299 To better understand which specific taxa from the *Proteobacteria* and *Bacteroidetes* increase in abundance on the
300 plant root, we quantified the contribution of each ASV to the first two PCos in **Figure 2e**. We visualized this
301 in a biplot that displays the top 25 ASVs that are most influential in differentiating the samples (**Supplementary**
302 **Figure 3**), and quantified which ASVs correlate most strongly with PCo1 (**Supplementary Table 2**). We found
303 that while *Streptomyces* and *Sphingomonas* ASVs most strongly influence the ordination, the abundance of the
304 proteobacterial genera *Massilia* and *Devosia* is strongly associated with PCo1, along which the samples from the
305 different compartments separated. *Massilia* constitutes a significant proportion of all *Proteobacteria* ($\sim 12.9 \pm 6.9\%$)
306 and was the most abundant genus in the RP1 communities ($\sim 7.4 \pm 4.4\%$). This indicates that *Massilia* and *Devosia*
307 are most enriched close to the roots and can be considered rhizosphere competent, i.e., capable of surviving
308 and thriving in the rhizosphere.
309



310
311
312
313
314

Figure 3 Proteobacteria and Bacteroidetes replace other phyla on the roots. a Average relative abundance of major phyla (>5% per compartment per experiment) minus their abundance in S in each soil-root compartment. b Relative abundance of major phyla. Remaining percentage of abundance is occupied by other phyla. Numbers on the x-axis indicate different experiments. Compartment abbreviations: soil (S), rhizosphere-4 (RS4), rhizosphere-3 (RS3), rhizoplane-2 (RP2) and rhizoplane-1 (RP1).

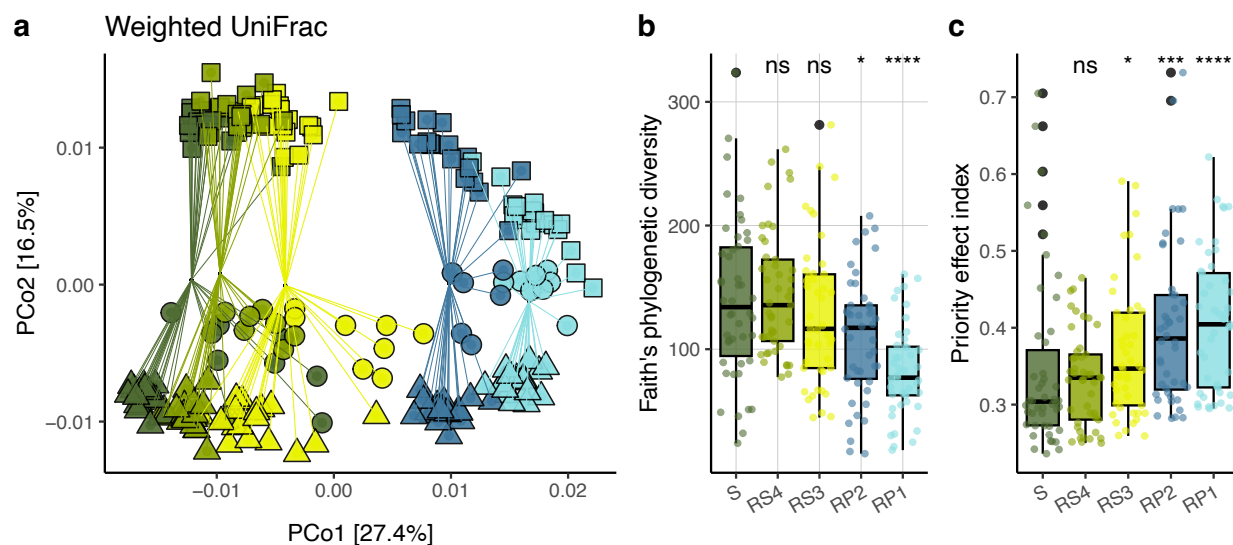
315
316
317
318
319
320
321
322
323
324
325
326
327
328
329
330
331
332
333
334
335
336

Rhizosphere microbiomes converge from diverse starting points

We observed that rhizosphere microbiomes become less diverse and more divergent from the soil microbiome as we move closer to the plant root (Figure 2), and that select taxa are repeatedly enriched along this soil-root gradient in different experiments (Figure 3; Supplementary Figure 3). Together, these results suggest that the enrichment of taxa towards the plant root is non-random and related to the genetic and functional similarity of the enriched taxa. To test this hypothesis, we calculated between-sample differences in taxonomic composition using the weighted UniFrac metric. As opposed to the previously used Bray-Curtis dissimilarity metric, which considers ASVs as categorical units, weighted UniFrac additionally incorporates the phylogenetic distances between ASVs, thereby accounting for their overall relatedness. When we then perform PCoA on these between-sample differences, we observed that samples from different experiments converged towards the roots (Figure 4a). Thus, the rhizosphere-associated microbes were phylogenetically similar in independent experiments, reflecting their genetic and functional similarity⁴². This is further supported by the decrease of Faith's phylogenetic diversity⁴³ (determined by summed branch lengths of the 16S rRNA V3-V4 amplicon-based phylogenetic tree) in the RP2 and RP1 samples, showing that communities near the roots contain phylogenetically more similar species than those in soil (Wilcoxon test, $p > 0.05$; Figure 4b). This suggests that the *Arabidopsis* rhizosphere is a selective environment consistently populated by a phylogenetically and likely functionally similar, competitive pool of microbes.

To further confirm the presence of a taxonomic signal across the soil-root gradient we quantified the degree of sample clustering by compartment that can be visually observed in the PCoA plots (Figure 3e, Figure 4a). To this end, we calculated the average Euclidian distance to the compartment centroid for each compartment using

337 both Bray-Curtis and weighted UniFrac metrics and combined those metrics into a so-called ‘priority effect
338 index’ by subtracting the weighted UniFrac values from those calculated using Bray-Curtis. A larger distance to
339 the compartment centroid indicates more variation between samples of the same compartment and suggests
340 that priority effects have played a larger role closer to the root. We found that the distance to the compartment
341 centroid increased slightly in the RS3 compartment, and more in the rhizoplane samples relative to S (Figure
342 4c; Wilcoxon test, $p < 0.05$). We hypothesize that priority effects play a role in root colonization, especially in
343 the rhizoplane, as phylogenetically related taxa that by chance arrive on the root first might have a competitive
344 advantage. This would cause samples to diverge on the individual or ASV level as these are functionally
345 redundant but converge on higher taxonomic ranks (Figure 4a).
346

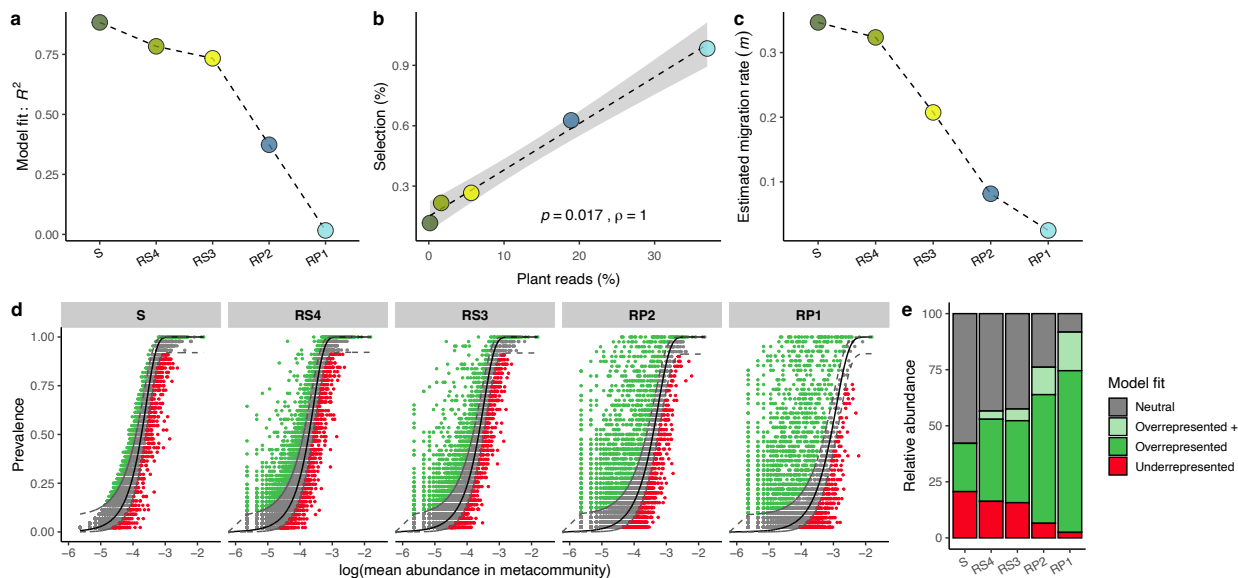


347
348 **Figure 4 Phylogenetic clustering of micro-organisms closer to the roots which appears to be driven by priority effects.** a PCoA
349 based on weighted UniFrac, which incorporates the phylogenetic distances between ASVs, thereby accounting for their relatedness. b
350 Faith's phylogenetic diversity (determined by summed branch lengths of the 16S rRNA V3-V4 amplicon-based phylogenetic tree) per
351 compartment. c Euclidian distances for all samples to the compartment centroid with the Bray-Curtis dissimilarity measure. A greater
352 distance to the centroid implies greater dissimilarity between communities, indicating a higher number of distinct ASVs that are present
353 between those samples. d Euclidian distances for all samples to the compartment centroid with the weighted UniFrac dissimilarity
354 measure, where phylogenetic relatedness of ASVs is considered. For all panels the Wilcoxon test was performed. * $p < 0.05$ ** $p < 0.01$
355 and **** $p < 0.0001$, ns = not significant. Compartment abbreviations: soil (S), rhizosphere-4 (RS4), rhizosphere-3 (RS3), rhizoplane-2
356 (RP2) and rhizoplane-1 (RP1).

357
358 Rhizosphere effect is associated with niche-based community assembly
359 Our results suggest that microbial communities near plant roots experience selective pressure, resulting in
360 phylogenetically similar communities. Thus far, the contribution of selection to the shaping of microbial
361 communities along the soil-root gradient has not been quantified. Four main ecological processes govern
362 microbial community assembly: selection, dispersal, drift, and speciation⁴⁴. Traditionally, biodiversity is
363 explained by niche theory, which proposes that each species has unique traits that allow it to occupy a specific
364 environment⁴⁵. This theory assumes that species are fundamentally different and can coexist because of these

365 differences. In contrast, neutral theory explains diversity as a balance between random dispersal, drift, and/or
366 speciation^{46,47}. Both niche and neutral processes can occur simultaneously in the assembly of local
367 communities⁴⁸. To investigate to what extent these processes contribute to rhizosphere microbiome assembly
368 along the soil-root gradient, we assessed the fit of the *Sloan Neutral Community Model for Prokaryotes* to the
369 distributions of ASVs in our soil-root gradient data²⁵. In short, the model predicts that, under a neutral sampling
370 process, taxa that are abundant in the metacommunity are also widespread in local communities, while rare taxa
371 are likely to be lost due to ecological drift²⁶. Here, for each compartment, we compare the observed prevalence
372 of ASVs (percentage of samples in which an ASV occurs) in the local root-compartments to their relative
373 abundance in the summed bulk soil samples, using a β -distribution where the parameter m is fitted.
374

375 The model fit varied between compartments, with a considerably lower fit for the washed ‘rhizoplane’ roots
376 (RP2 and RP1) compared to the ‘rhizosphere’ compartments (RS4 and RS3; **Figure 5a**). A lower model fit
377 indicates that community composition is primarily non-neutral, i.e., driven by selection, or non-random
378 dispersal or speciation, although the latter process is likely not relevant in our 21-day experiment. The model
379 fit was almost zero for RP1 samples, indicating that the microbial communities in this compartment are strongly
380 selected for or dispersal enriched. The estimated migration rate m decreased towards the root, suggesting that
381 microbial communities near the roots are not shaped by dispersal from the bulk soil, but rather by reproduction
382 and replacement from within the local community (**Figure 5b**). The model fit was positively correlated with
383 the percentage of plant reads (**Figure 5c**). In all compartments, there were ASVs that occurred more or less
384 frequently than predicted by the neutral model (referred to as over- and underrepresented ASVs, respectively)
385 and ASVs that followed the distribution of the neutral model (**Figure 5d** and e). For a small subset of ASVs a
386 model fit could not be determined (from 3.7% in RS4 samples to 17.2% in RP1 samples, light green parts in
387 **Figure 5d**), since those ASVs were below the detection limit or absent from S samples that were used as the
388 seeding metacommunity in this analysis. Therefore, we assumed that these ASVs were also overrepresented in
389 root-associated compartments compared to the bulk soil, although we kept them separate for additional analysis
390 and refer to them as ‘overrepresented +’. While the model fit was similar for the RS4 and RS3 compartments,
391 the migration rate m was lower for RS3. RS3 contains more ASVs with a larger positive deviation from the
392 neutral model than RS4 (**Figure 5d**), meaning that their prevalence is higher than expected according to neutral
393 processes. This indicates that while selection is equally important in RS4 and RS3, priority effects may play a
394 bigger role in RS3 and there is less immigration than in RS4. All in all, microbial community composition near
395 plant roots is primarily driven by selection, priority effects play an important role, and immigration from bulk
396 soil is limited.
397



398

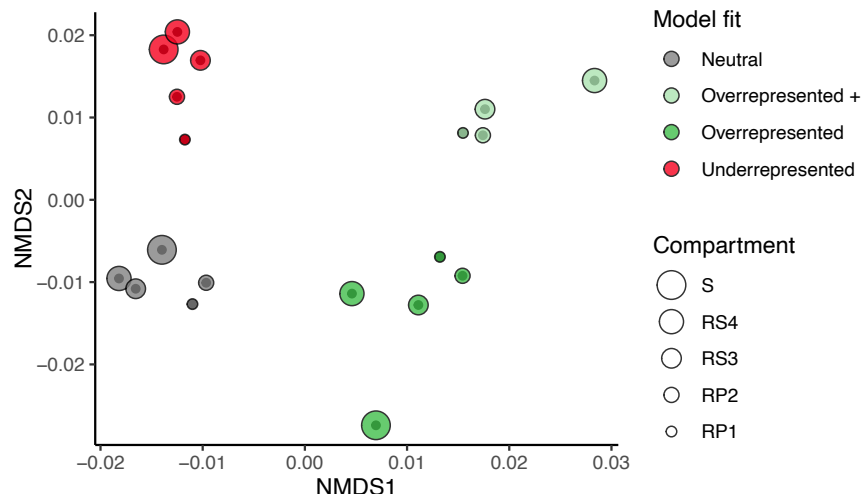
399 **Figure 5 Selection-based community processes become more important closer to the root.** **a** Neutral model fit (generalized R^2)
 400 per compartment. A higher neutral model fit means less influence of selection-based community assembly processes. **b** Estimated
 401 migration rate per compartment. **c** The importance of selection, represented by the R^2 of the model fit, as a function of the distance to
 402 the root, proxied by the number of plant reads per compartment (Spearman, $p = 0.017, \rho = 1$). **d** Prevalence in compartment samples
 403 as a function of abundance in the bulk soil for each ASV per compartment, coloured by model fit. **e** The percentage of overrepresented
 404 ASVs (dark and light green bars) increases as distance to the root decreases, i.e., a larger part of the microbial community behaves non-
 405 neutral, suggesting a larger rhizosphere effect. Compartments are indicated by abbreviations: soil (S), rhizosphere-4 (RS4), rhizosphere-
 406 3 (RS3), rhizoplane-2 (RP2) and rhizoplane-1 (RP1).

407

408 Phylogenetically similar microbes selected along the gradient

409 The proportion of overrepresented ASVs increased near the root, while that of the underrepresented ASVs,
 410 and ASVs that followed the neutral distribution decreased (**Figure 5e**). Neutrally distributed taxa are primarily
 411 generalists, widespread genera with opportunistic growth strategies, while taxa that are positively selected for
 412 are likely specialists adapted to a specific environment⁴⁹. Therefore, we expected that the phylogenetic
 413 composition of the over- and underrepresented ASVs was different from the microbes whose abundances were
 414 described well by the model. To investigate this, we performed Non-metric Multidimensional Scaling (NMDS)
 415 analysis using the weighted UniFrac metric to visualize differences in community structure among the partitions
 416 of ASVs with different model fits per compartment (**Figure 6**). Pair-wise permutation analysis (999
 417 permutations) revealed that all partitions had a distinct microbial community (PERMANOVA, $p < 0.05$). The
 418 phylogenetic composition of the partitions that diverged from neutral patterns remained relatively similar across
 419 the soil-root gradient, despite the changing composition of compartment communities as a whole. Among the
 420 overrepresented microbes are those genera that we identified previously that align well with the soil-root
 421 gradient, e.g. *Massilia* and *Niastella*. An interesting overrepresented+ genus is *Pseudomonas*, a well-known root
 422 coloniser⁵⁰⁻⁵⁵. Although *Pseudomonas* was not detected in bulk soil samples, several ASVs were found in RS3 and
 423 RP1 samples. Overall, taxa that get selected on the root are already visible in compartments further away from

424 the root, albeit less abundant. Thus, although the rhizosphere effect is not yet clearly visible in the RS4 samples,
425 a part of the microbes in this compartment is already influenced by the plant root and its exudates.
426



427
428 **Figure 6 ASVs that are selected for or against along the soil-root gradient are phylogenetically distinct from ASVs that follow**
429 **a neutral distribution.** Partitions of overrepresented ASVs are shown in light and dark green, underrepresented ASVs in red and
430 neutrally distributed ASVs in grey. Shape size indicates compartment, smaller symbols indicate less sampled soil. Compartment
431 abbreviations: soil (S), rhizosphere-4 (RS4), rhizosphere-3 (RS3), rhizoplane-2 (RP2) and rhizoplane-1 (RP1).

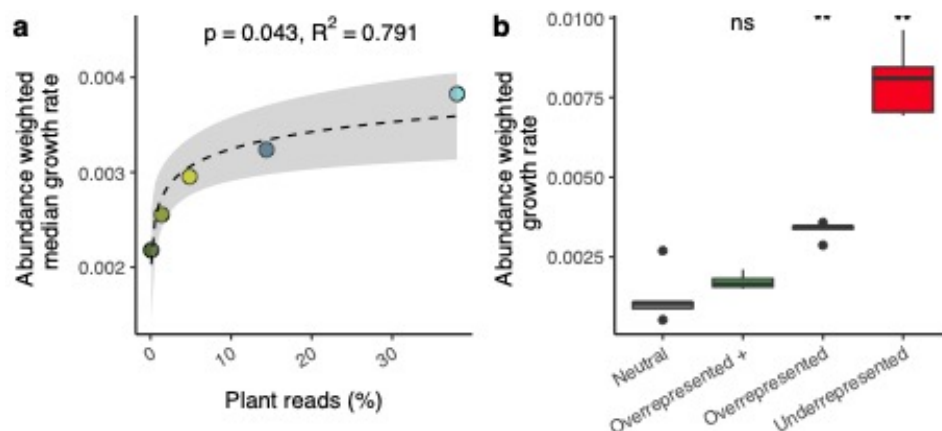
432
433 Rhizosphere microbes might use different growth strategies

434 Most microbes living in the proximity of plant roots are so-called 'r-strategists': copiotrophs that have high
435 nutritional requirements and can exhibit high growth rates when resources are abundant⁵⁶. Nutrient levels are
436 higher in the rhizosphere compared to the bulk soil due to the secretion of compounds by plant roots. As a
437 result, the concentration of nutrients is typically represented by a gradient, being the highest near the root and
438 decreasing further away. Given our sampling strategy, we expected the average growth rate potential to go up
439 gradually along the soil-root nutrient gradient, inversely related to root distance. We recently showed that
440 rhizosphere-associated bacteria typically display higher growth rate potential and encoded more mobility
441 mechanisms than soil bacteria, partly explaining their ability to reach and proliferate in the rhizosphere³⁷. To
442 assess whether growth rate potential can be modelled as a function of the distance to the root in addition to
443 comparing the different biomes, we compared the median predicted minimal doubling time (PMDT) for each
444 genus in our dataset (see Methods). For each compartment, we calculated the median PMDT as a weighted
445 median of all PMDT values for all genera weighted by their relative abundances, and plotted them against the
446 amount of plant reads as a proxy for root distance. We found that the growth rate potential of the microbiota
447 was the highest in the two 'rhizoplane' compartments (RP2 and RP1) and ~1.5 times higher than in S (Wilcoxon
448 test, $p < 0.01$). The increase in growth rate potential in these rhizoplane compartments was effectively the
449 largest, corroborated by the significant log-linear model fit (Linear model, $\log(y) \sim x$, $p = 0.043$, $R^2 = 0.791$;

450 **Figure 7a).** Growth rate potential flattens out towards the root, indicating that the maximum growth rate
451 potential is reached. These results corroborate our earlier results that root-associated communities are enriched
452 in microbes with a high growth rate potential compared to bulk soil³⁷ and that the largest increase can be
453 observed in the rhizosphere compartment.

454
455 Most likely, not only copiotrophs are able to survive in proximity of the root, but microbes can also use other
456 strategies to colonize the rhizosphere and outcompete others. Therefore, we calculated the abundance-weighted
457 median growth rate potential of taxa for the groups of ASVs based on their neutral model fits to assess whether
458 over- and/or underrepresentation of microbes is linked to their respective growth rate potential. We found that
459 the group of ASVs that were underrepresented in the root-associated compartments had the highest growth
460 rate potential: ~6.5 times higher than the neutrally distributed ASVs (**Figure 7b**; Wilcoxon test, $p = 0.008$).
461 These microbes are less prevalent on the root than expected based on their abundance in soil, likely due to
462 competition, mutual inhibition or by low tolerance to plant root-excreted antimicrobial compounds like
463 coumarins³⁹. Thus, being a potential fast grower is not sufficient to thrive in the rhizosphere, potentially due to
464 competition with other fast growers. They might, however, still manage to colonize the root because they are
465 generalist species that can survive in a wide range of environments⁵⁷. In terms of their growth rate potential,
466 the underrepresented ASVs were followed by ASVs that were overrepresented in the root-associated
467 compartments with average growth rate potential ~2.5 times higher than neutrally distributed ones (Wilcoxon
468 test, $p = 0.008$). Overrepresented ASVs make up the largest proportion of bacteria in the ‘rhizoplane’
469 compartments, and likely complement their relatively high growth rate potential with other traits that make
470 them highly rhizosphere competent. Interestingly, genera within the overrepresented+ class had similar growth
471 rate potential as the ASVs whose distribution followed the neutral model (Wilcoxon test, $p > 0.05$). While these
472 ASVs were not detected in the bulk soil and are predicted to be relatively slow growers, they are still able to
473 colonize the root in high numbers (**Error! Reference source not found.**). These microbes, amongst them the p
474 previously noted genus *Massilia*, are probably specialist species that have specific traits not related to their growth
475 rate potential, like competitive ability, that help them survive and thrive in the rhizosphere.

476



477

478 **Figure 7 Growth rate potential increases closer to the roots, but rhizosphere-competent microbes have different growth**
479 **strategies.** a Abundance-weighted median growth rate potential per compartment is significantly correlated with the percentage of
480 plant reads (Linear model, $\log(y) \sim x$, $p = 0.043$, $R^2 = 0.791$). 'Rhizoplane' compartment microbes have on average a higher median
481 growth rate potential as compared to bulk soil microbes (Wilcoxon, $p < 0.01$). b Abundance-weighted growth rate potential for microbes
482 categorized by their neutral model fit. Compared to neutrally distributed microbes, microbes that are over- and underrepresented in the
483 root-associated compartments display higher median growth rate potential (Wilcoxon test, $p = 0.008$).

484

485 Discussion

486

487 In this study, we employed a reproducible sampling approach to harvest the roots and adhering soil of individual
488 *Arabidopsis* plants cultivated in different soil batches. Using increasingly stringent cleaning and washing steps,
489 we sampled the soil-to-root continuum in five consecutive compartments, including the unplanted bulk soil
490 itself. This enabled us to investigate microbial community composition and community assembly processes
491 along this continuum with high resolution, gaining critical insights in the microbial dynamics in this hotspot of
492 microbial activity. As we move closer to the root, we observed that bacteria from the *Proteobacteria* and
493 *Bacteroidetes* replaced other phyla and that microbes that were below the detection limit in soil can be the most
494 abundant species in the rhizosphere or rhizoplane. Despite different initial soil microbiomes, rhizosphere and
495 rhizoplane microbiomes converge when we considered microbial phylogenetic relatedness, supporting earlier
496 work showing that specific bacterial families and genera are repeatedly associated with plant roots¹⁹. It also
497 shows that plant roots impact their local environment in a robust and reproducible manner, exerting selective
498 pressure on the surrounding microbes likely to their own benefit. Nevertheless, we also observed that, in
499 addition to selection pressure- or niche-based community assembly, also priority effects and alternative growth
500 strategies can contribute to shaping the rhizosphere microbiome.

501

502 **Comparative analysis of the rhizosphere microbiome across plants, soils and samples requires**
503 **reproducible sampling**

504 Our findings highlight the importance of careful consideration when sampling roots in rhizosphere studies.
505 Different sampling methods can lead to varying conclusions regarding the strength of the rhizosphere effect
506 and its root-associated microbiome and assembly processes. In the current study, α -diversity was significantly
507 lower in the 'rhizoplane' compartments when compared to bulk soil. We expect that the reduction in α -diversity
508 is accompanied by a reduction in functional gene richness, as taxonomic and functional diversity are inherently
509 linked⁵⁸. The same effect was seen for β -diversity, as the community composition diverged from bulk soil while
510 closing in on the root. More importantly, both diversity parameters correlated significantly with the distance to
511 the root – approximated in our study by the number of plant-derived reads – emphasizing the need to treat the
512 rhizosphere as an environmental continuum or gradient. Earlier cultivation-dependent and -independent
513 studies recognized lower α - and higher β -diversity in the rhizosphere compared to bulk soil, but to what extent
514 depended heavily on the sampling method. In studies on *Arabidopsis*, analysis of species richness – a proxy for
515 α -diversity – in the rhizosphere compartment displayed a slight decrease⁵⁹ or no change at all^{19,22,60,61}. More
516 often, α -diversity decreased significantly only when examining the rhizoplane or the endophytic
517 compartment^{18,19,60,61}, which compares best to our 'rhizoplane' compartments RP2 and RP1⁷¹. In an earlier
518 study on the *Arabidopsis* rhizosphere effect, rhizosphere and endophytic communities were found both to be
519 different from bulk soil, and this effect was largest for the endophytic community¹⁹. The compartment effect
520 found in Lundberg et al. (2012) (rhizosphere vs. endosphere) aligned well with the largest principal component
521 of the PCoA. Comparable to the variation between our different experiments, soil batch was represented by
522 the second principal component¹⁹. These findings are comparable to results from Bulgarelli and co-authors
523 (2012). Here, analysis of sample-to-sample β -diversity revealed that all root samples were distinct from
524 rhizosphere and bulk soil samples, irrespective of soil type. For rhizosphere and soil samples this distinction
525 was less clear¹⁸. Two other studies that compared the rhizosphere and endosphere show similar trends: the
526 difference between rhizosphere and soil microbiomes (based on the PERMANOVA-test R^2) was relatively
527 small, while for the endosphere-soil comparisons R^2 -values were larger, indicating more dissimilar
528 communities^{22,61}. Our rhizoplane-to-soil β -diversity compartment effect sizes are smaller than those reported
529 by Schnejderberg et al.²², likely due to the spread between samples of different experiments. Experiment-
530 specific R^2 values ranged from 0.42 – 0.72 for RP1 samples, which are comparable to theirs.
531

532 **Rhizosphere-competent *Massilia* species are rare in soil, yet abundant on plant roots and understudied**
533 The gradual change in community composition along the soil-root gradient was mostly caused by a doubling
534 in abundance of *Proteobacteria* closer to the roots. Members of this phylum include fast-growing, generalist *r*-
535 strategists that do well in environments where organic resources are abundant⁵⁶. They are often found enriched
536 on the roots of *Arabidopsis*^{18,19,21,22,62} and many other plants including crops like maize^{63,64} and wheat^{65–67}.
537 Within the *Proteobacteria*, we found members of the *Betaproteobacteria* to increase in particular, and within this
538 class, the family *Oxalobacteraceae* was most prominent. *Oxalobacteraceae* are good rhizosphere and even better

539 endosphere colonizers^{18,60}. Of these, the genus *Massilia* correlated most strongly with the first axis in our PCoA
540 which distinguished samples of different compartments. It was nearly absent in the bulk soil, but
541 overrepresented closer to the roots where it occurred in high abundance. *Massilia* species are generally good
542 colonizers of biological surfaces, and often found enriched in the rhizosphere^{21,52,62,67}. They associate mostly
543 with older parts of the plant root⁶⁸, suggesting that they do not necessarily need highly metabolically active cells
544 for survival. This might give them a competitive advantage over other microbes that need to be in proximity to
545 root tips to grow. Our fine-grained sampling focused on complete roots of 4-week-old *Arabidopsis* plants, and
546 we are thus unable to differentiate microbial communities from young or older parts of the roots. However,
547 *Massilia* species have been reported to display typical plant-growth-promoting capabilities⁶⁸ in association with
548 older root tissues. For example, in nitrogen-poor soil, *Massilia* isolates were able to promote maize shoot growth
549 and nitrogen accumulation with induction of lateral root formation in lateral rootless mutants⁶⁹, a process that
550 takes place in the older parts of the root. A specific *Massilia* ASV was found to be associated with pathogen-
551 infected *Arabidopsis* plants⁷⁰, and it was also identified as a 'hub' species in the wheat rhizosphere, suggesting
552 it plays an essential role in the assembly and functionality of plant-associated communities⁶⁷. *Oxalobacteraceae*,
553 and specifically the genus *Massilia*, are extremely rhizosphere competent and might fulfil essential functions
554 within the rhizosphere microbiome. To date only 139 *Massilia* spp. genome sequences are deposited in the
555 NCBI GenBank database. Compared with well-known, and well-studied rhizosphere-competent genera like
556 *Bacillus* (9,322 genomes), *Pseudomonas* (8,000 genomes excluding the opportunistic human pathogen *Pseudomonas*
557 *aeruginosa*), *Rhizobium* (1,500 genomes), and *Agrobacterium* (697 genomes) this highlights our limited
558 understanding and characterization of this genus. Such is further corroborated by the much smaller number of
559 scientific studies that can be found via NCBI PubMed and that evaluated the interaction between members of
560 the *Massilia* genus and plants (1,198 studies) as compared to that involving abovementioned genera (*Pseudomonas*:
561 106,543; *Bacillus*: 100,729; *Agrobacterium*: 51,095; *Rhizobium*: 20,302 studies).

562

563 **Deterministic processes drive root microbial community assembly**

564 Our research points towards niche-based community assembly processes driving the rhizosphere effect,
565 resulting in phylogenetically similar microbial communities on the root. These consist for an important part of
566 organisms from fast-growing generalist taxa³⁷. Few studies try to quantify microbial community assembly in the
567 root environment, and results are variable. One study on the soybean rhizosphere suggested that bulk soil
568 microbiomes were governed solely by neutral processes, whereas rhizosphere samples showed deterministic
569 dynamics⁷¹. Another study, also on soybean rhizospheres, found that deterministic processes were more
570 important in bulk soil than in the rhizosphere and endosphere³⁰. A third soybean study found that neutral
571 processes shaped rhizo- and endosphere microbiomes, although those were not compared to bulk soil
572 samples⁷². In long-term cultivated wheat, Fan and co-authors (2017) found that deterministic assembly
573 processes dominated bacterial community composition in plant and soil compartments²⁹. All these studies used

574 different methods to quantify the importance of niche and neutral community assembly processes, including
575 differences in sampling strategy and analysis, so a one-to-one comparison is complicated. We expect that
576 extending our approach of incrementally sampling the rhizosphere to other plant species, will help elucidate
577 not only what assembly processes dominate the rhizosphere, but also what microbes are selected for or against.
578

579 **Priority effects drive compartment differentiation across plants and experiments**

580 When we conducted PCoA using various β -diversity metrics, samples clustered by noticeably different patterns.
581 Samples from the three different experiments diverged in compartments closer to the root when we used Bray-
582 Curtis, but not when we used weighted UniFrac. This means the number of different ASVs increased, while
583 their phylogenetic diversity remained stable from soil to root. Additionally, the neutral model predicted that
584 migration rates decreased near the roots, indicating that there is enhanced growth of the local community and
585 less migration from the bulk soil. This is consistent with the higher growth rate potential of rhizosphere-
586 associated bacteria³⁷ and highlights the importance of priority effects in the colonization of the rhizosphere⁷⁴.
587 Using synthetic communities and sequential inoculations, Wippel and co-authors (2021) showed that the order
588 of arrival was indeed a major factor determining the final microbial community on *Arabidopsis* and *Lotus japonicus*
589 roots⁶¹. The effect of secondary inoculations on the community depended on the context, e.g., the origin of the
590 inoculated community, the plant compartment, and the nutritional status of the plant, which might all influence
591 the competitive ability of present microbes. Thus, understanding the effects of timing on rhizosphere
592 community assembly will be crucial for gaining a complete picture of these complex systems.
593

594 In conclusion, our study investigated the rhizosphere effect in *Arabidopsis* along a soil-root gradient, utilizing
595 three distinct experiments with comparable sampling methods. Microbial communities displayed a gradual shift
596 in composition along the gradient, with *Proteobacteria* and *Bacteroidetes* dominating the rhizoplane compartments.
597 The rhizosphere effect, indicated by decreasing α -diversity and distinct β -diversity patterns, strengthened
598 towards the root. The enrichment of specific taxa on roots, such as *Massilia* and *Devosia*, revealed phylogenetic
599 clustering and suggested a non-random selection of microbes. Priority effects became more pronounced closer
600 to the root, influencing community structure. Modelling using the Sloan Neutral Community Model indicated
601 that the root-associated communities were primarily shaped by non-neutral processes like selection, with
602 priority effects playing a larger role in compartments with limited migration from bulk soil. Additionally, growth
603 rate potential analysis suggested that taxa that were underrepresented on the root had the highest growth rate
604 potential, emphasizing the complex interplay of (growth) strategies in the rhizosphere. Our discoveries advance
605 our comprehension of the intricate dynamics involved in rhizosphere microbiome assembly, underscoring the
606 critical role of sampling strategies. This insight is particularly pertinent for future research delving into plant-
607 microbe interactions, highlighting the significance of methodological approaches in unraveling the complexities
608 of the rhizosphere microbiome.

609 Acknowledgements

610

611 The authors would like to express their gratitude to the members of the Utrecht University Plant-Microbe
612 Interactions lab and Metagenomics Group (MGX) for their valuable discussions. We acknowledge the Utrecht
613 Sequencing Facility (USEQ) for providing sequencing service and data. USEQ is subsidized by the University
614 Medical Center Utrecht and The Netherlands X-omics Initiative (NWO project 184.034.019). This study was
615 supported by the NWO Green II Grant no. ALWGR.2017.002 (S.W.M.P., J.J.S.G., R.d.J.) and the Novo
616 Nordisk Foundation Grant no. NNF19SA0059362 (R.d.J.). B.E.D. was supported by the European Research
617 Council (ERC) Consolidator grant 865694: DiversiPHI, the Deutsche Forschungsgemeinschaft (DFG, German
618 Research Foundation) under Germany's Excellence Strategy – EXC 2051 – Project-ID 390713860, and the
619 Alexander von Humboldt Foundation in the context of an Alexander von Humboldt-Professorship funded by
620 the German Federal Ministry of Education and Research.

621

622 Author contributions

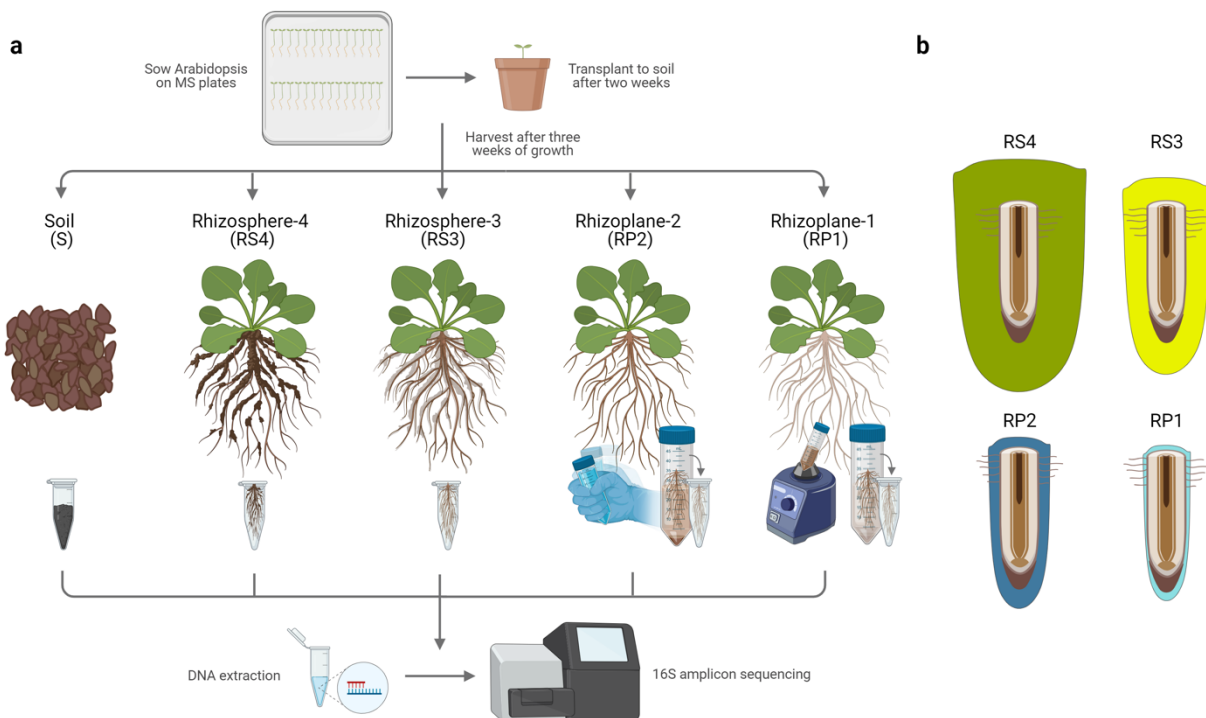
623

624 **Sanne W.M. Poppeliers:** Conceptualization, Methodology, Analysis, Visualization, Writing – Original Draft.
625 **Juan J. Sánchez-Gil:** Investigation, Writing: Review and Editing. **José L. López:** Analysis of growth rate
626 potential data. **Bas E. Dutilh:** Supervision, Funding acquisition, Writing: Review and Editing. **Corné M.J.**
627 **Pieterse:** Supervision, Funding acquisition, Writing: Review and Editing. **Ronnie de Jonge:** Supervision,
628 Project administration, Funding acquisition, Writing – Review and Editing.

629

630 **Supplementary material**

631



632

633 **Supplementary Figure 1 Schematic overview of the experimental setup of the rhizosphere effect experiments.** a Surface-
634 sterilized Arabidopsis seeds were sown on plates with Murashige and Skoog medium. After two weeks seedlings were transplanted to
635 soil and grown for another three weeks until harvest. Unplanted samples were considered bulk soil (S). About 0.25g of soil was taken
636 per pot. Then, for all root compartments, roots were harvested in different ways and collected in 2-mL Eppendorf tubes. For
637 rhizosphere-4 samples (RS4), roots were taken out of the soil and gently shaken until most loose soil fell off. This compartment
638 contained the widest zone of soil environment around the roots and its microbial community is likely to show the closest resemblance
639 to that of the bulk soil. For rhizosphere-3 (RS3), roots were harvested similarly, but additionally they were cleared of most loose soil by
640 tapping them on paper and stripping them from soil as much as possible. The rhizoplane-2 (RP2) roots were harvested as RS3, and
641 additionally gently shaken in a 10 mM MgSO₄ solution. For rhizoplane-1 (RP1), roots were additionally vortexed twice in a phosphate-
642 Silwet buffer. As a result, in each consecutive compartment from RS4 to RP1 we sampled bacterial communities more closely associated
643 with the root, or not influenced by the root at all (S). We consider that RS4 and RS3 may be compared to what other studies often refer
644 to as 'rhizosphere', while RP2 and RP1 could be considered 'rhizoplane'. Notably, our sampling strategy also included the roots
645 themselves, sometimes referred to as 'endosphere'. b Schematic view of how the sampling strategy results in a gradual decrease in soil
646 and microbes attached to the roots.

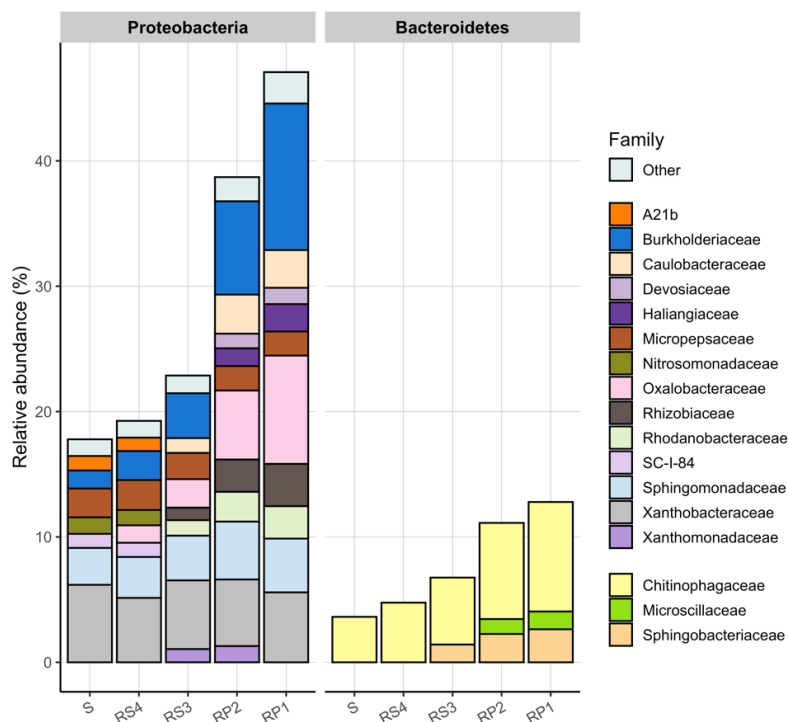
647

648 **Supplementary Table 1 Amount of plant reads increases towards the roots.** Dunn's post-hoc test results after Kruskal-Wallis test
649 comparing the amount of plant reads between neighbouring compartments. For Exp1, differences between neighbouring compartments
650 are smaller, therefore not significant (Figure 2b).

	Compartment 1	Compartment 2	Corrected p-value
Exp1	S	RS4	0.1175
	RS4	RS3	0.1188
	RS3	RP2	0.1094
	RP2	RP1	0.1752
Exp2	S	RS4	0.0201
	RS4	RS3	0.0204

	RS3	RP2	0.0168
	RP2	RP1	0.0303
Exp3	S	RS4	0.0215
	RS4	RS3	0.0307
	RS3	RP2	0.0233
	RP2	RP1	0.0225

651
652



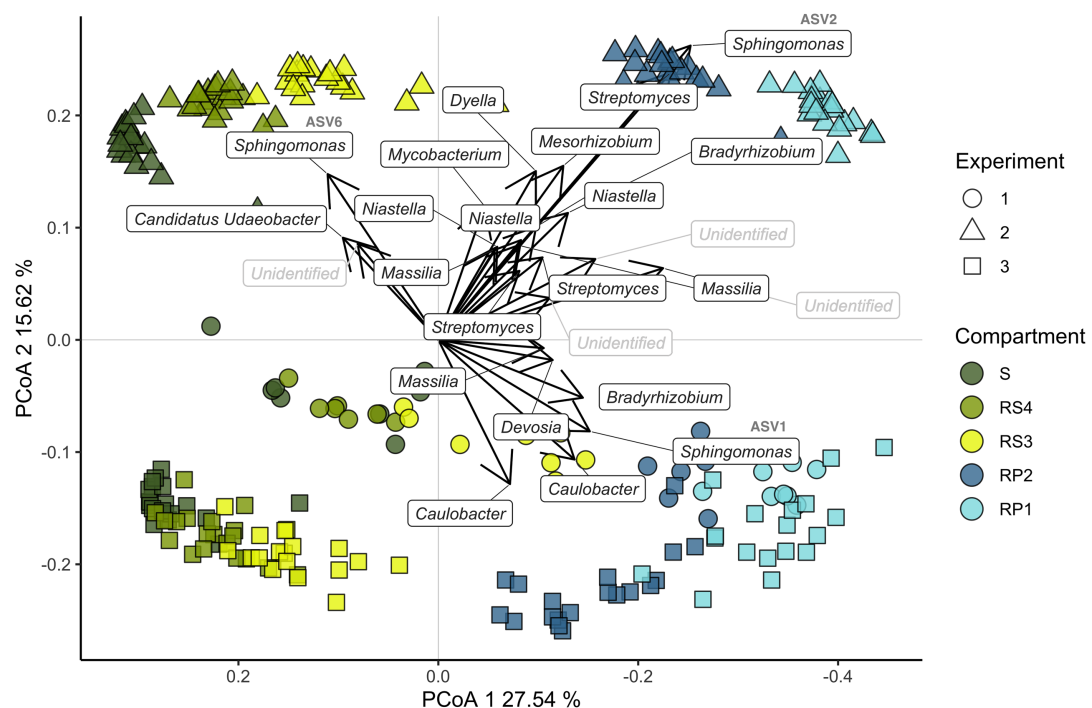
659
660
661

Supplementary Table 2 *Massilia* and *Devosia* ASVs most strongly associated with the rhizosphere effect. Absolute PC2-values indicate how strong an ASV correlates with PC1. The table is ranked from highest to lower correlation.

FeatureID	Family	Genus	PC2	abs(PC2)
658a6c3cb0afc78acc734563c04ed34f	<i>Oxalobacteraceae</i>	<i>Massilia</i>	-0.0007322	0.00073221
c7511f6ef1f1bdb63c249524f83d76e9	<i>Devosiaceae</i>	<i>Devosia</i>	-0.0017991	0.00179906
85260e58dbf4faee8413ec1468207eb4	<i>Ktedonobacteraceae</i>	<i>Unidentified</i>	0.00373465	0.00373465
9db2817f5c42be6a7bcbca662959982d	<i>Xanthobacteraceae</i>	<i>Bradyrhizobium</i>	-0.0051554	0.00515542
73685289bc86236f252522bc1bacf0da	<i>Streptomycetaceae</i>	<i>Streptomyces</i>	0.00614565	0.00614565
00f3a4a2243093399302c8ce5667b076	<i>Burkholderiaceae</i>	<i>Unidentified</i>	0.00638785	0.00638785
51fbe3718b46cca351549f2b7972fc7b	<i>Burkholderiaceae</i>	<i>Unidentified</i>	0.00720283	0.00720283

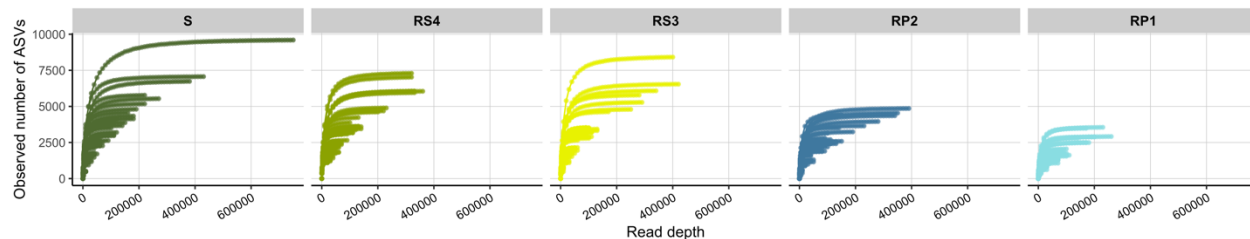
6c8e8f15c8b62edfc17dd5fc30ecd8cd	<i>Streptomycetaceae</i>	<i>Streptomyces</i>	0.00734874	0.00734874
b0e887d50801f758fdfbf1821653915	<i>Oxalobacteraceae</i>	<i>Massilia</i>	0.00805801	0.00805801
dd8c8d60bfca3e1df01a4bbff8d3326e	<i>Sphingomonadaceae</i>	<i>Sphingomonas</i>	-0.0081524	0.00815244
63069a5cca4f5ce4e0d25536867087f5	<i>Chitinophagaceae</i>	<i>Niastella</i>	0.0082916	0.0082916
84cfb99ca8d2e841b7fdd082092d4c5e	<i>Oxalobacteraceae</i>	<i>Massilia</i>	0.00842833	0.00842833
1b039cf1f64eef764da543c4f8f30d7	<i>WD2101 soil group</i>	<i>Unidentified</i>	0.00855884	0.00855884
47dc1c5b77e91c1fc706a7204175af8a	<i>Chitinophagaceae</i>	<i>Niastella</i>	0.00889172	0.00889172
011ac4ce13db0a5672151faea73477f0	<i>Chthoniobacteraceae</i>	<i>Candidatus Udaeobacter</i>	0.00910402	0.00910402
59ac5c6a9cb3c4658d91b4ec00717fe3	<i>Chitinophagaceae</i>	<i>Niastella</i>	0.01007207	0.01007207
fc672ff88dc475b143532167712d4329	<i>Caulobacteraceae</i>	<i>Caulobacter</i>	-0.0106656	0.01066565
fb75fa1fac5ad54c9d64c653e50a7126	<i>Xanthobacteraceae</i>	<i>Bradyrhizobium</i>	0.01131134	0.01131134
d019faf316527e1c1a5e77779455abee	<i>Mycobacteriaceae</i>	<i>Mycobacterium</i>	0.01193138	0.01193138
52d6fae91fe613402b5eb064db422d2a	<i>Caulobacteraceae</i>	<i>Caulobacter</i>	-0.0128518	0.0128518
8d2a29d23de2d1b6cada06bf85915274	<i>Sphingomonadaceae</i>	<i>Sphingomonas</i>	0.0147735	0.0147735
399e2afe75e1225bfc99f49570bc0cdb	<i>Rhodanobacteraceae</i>	<i>Dyella</i>	0.0150431	0.0150431
9554c4285d3f4f6e7e9384b5d21b3274	<i>Rhizobiaceae</i>	<i>Mesorhizobium</i>	0.01550845	0.01550845
93120265f9c84ff7e35370a1f4336272	<i>Streptomycetaceae</i>	<i>Streptomyces</i>	0.02380364	0.02380364
2345c975ae95fddd8aa7816acb912ffc	<i>Sphingomonadaceae</i>	<i>Sphingomonas</i>	0.02622475	0.02622475

662



663
664
665
666
667
668

Supplementary Figure 3 *Massilia* and *Devosia* strongly associated with rhizoplane compartments, while *Sphingomonas* contributes most to the ordination. PCoA biplot using the Bray-Curtis distance metric where arrows show the 25 ASVs that contribute most to the ordination. The longer the arrow the larger the contribution. Arrows that align best with PCoA1 (grey line) are correlated strongest with the soil-root gradient. Compartments are indicated by abbreviations: soil (S), rhizosphere-4 (RS4), rhizosphere-3 (RS3), rhizoplane-2 (RP2) and rhizoplane-1 (RP1). 'Unidentified' taxa are not classified on the genus level.



669

670 **Supplementary Figure 4 Saturation is nearly reached in almost all samples.** Rarefaction curve for all samples, coloured by
671 compartment.

672

673 **Supplementary Table 3 Phasing primers used for amplification of the hypervariable V3-V4 region of the 16S rRNA gene.**

50-NGS1-16s-N701	TCGTCGGCAGCGTCAGATGTGTATAAGAGACAGTCGCCCTACCTGTGGCCTACGGGNGGCWGCAG
51-NGS1-16s-N702	TCGTCGGCAGCGTCAGATGTGTATAAGAGACAGCTAGTACGGAGTGGCCTACGGGNGGCWGCAG
52-NGS1-16s-N703	TCGTCGGCAGCGTCAGATGTGTATAAGAGACAGTTCTGCCCTGCGACCTACGGGNGGCWGCAG
53-NGS1-16s-N704	TCGTCGGCAGCGTCAGATGTGTATAAGAGACAGGCTCAGGAATGACCTACGGGNGGCWGCAG
54-NGS1-16s-N705	TCGTCGGCAGCGTCAGATGTGTATAAGAGACAGAGGAGTCCCACCTACGGGNGGCWGCAG
55-NGS1-16s-N706	TCGTCGGCAGCGTCAGATGTGTATAAGAGACAGCATGCCCTACGACCTACGGGNGGCWGCAG
56-NGS1-16s-N707	TCGTCGGCAGCGTCAGATGTGTATAAGAGACAGGTAGAGAGGGCTACGGGNGGCWGCAG
57-NGS1-16s-N708	TCGTCGGCAGCGTCAGATGTGTATAAGAGACAGCCTCTGGCCTACGGGNGGCWGCAG
58-NGS1-16s-N709	TCGTCGGCAGCGTCAGATGTGTATAAGAGACAGAGCGTAGCTCTACGGGNGGCWGCAG
59-NGS1-16s-N710	TCGTCGGCAGCGTCAGATGTGTATAAGAGACAGCAGCCTCGTCTACGGGNGGCWGCAG
60-NGS1-16s-N711	TCGTCGGCAGCGTCAGATGTGTATAAGAGACAGTGCCTTCCCTACGGGNGGCWGCAG
61-NGS1-16s-N712	TCGTCGGCAGCGTCAGATGTGTATAAGAGACAGTCCTTACCCCTACGGGNGGCWGCAG
62-NGS1-16s-N501	GTCTCGTGGGCTCGGAGATGTGTATAAGAGACAGTAGATGCCACTTCTGACTACHVGGGTATCTAATCC
63-NGS1-16s-N502	GTCTCGTGGGCTCGGAGATGTGTATAAGAGACAGCTCTATTCTGACTACHVGGGTATCTAATCC
64-NGS1-16s-N503	GTCTCGTGGGCTCGGAGATGTGTATAAGAGACAGTATCCTCTACTCAGACTACHVGGGTATCTAATCC
65-NGS1-16s-N504	GTCTCGTGGGCTCGGAGATGTGTATAAGAGACAGAGAGTAGAGATAGACTACHVGGGTATCTAATCC
66-NGS1-16s-N505	GTCTCGTGGGCTCGGAGATGTGTATAAGAGACAGGTAGAGCTAGACTACHVGGGTATCTAATCC
67-NGS1-16s-N506	GTCTCGTGGGCTCGGAGATGTGTATAAGAGACAGACTGCATATCGACTACHVGGGTATCTAATCC
68-NGS1-16s-N507	GTCTCGTGGGCTCGGAGATGTGTATAAGAGACAGAAGGAGTAAGACTACHVGGGTATCTAATCC
69-NGS1-16s-N508	GTCTCGTGGGCTCGGAGATGTGTATAAGAGACAGCTAACGCTGACTACHVGGGTATCTAATCC

674

675

676 References

677

678 1. Chaparro, J. M. *et al.* Root exudation of phytochemicals in *Arabidopsis* follows specific patterns that are developmentally
679 programmed and correlate with soil microbial functions. *PLoS One* **8**, e55731 (2013).

680 2. Kuzyakov, Y., Raskatov, A. & Kaupenjohann, M. Turnover and distribution of root exudates of *Zea mays*. *Plant and Soil* **2003**
681 **254**: 254, 317–327 (2003).

682 3. Kuzyakov, Y. & Razavi, B. S. Rhizosphere size and shape: temporal dynamics and spatial stationarity. *Soil Biol Biochem* **135**,
683 343–360 (2019).

684 4. Gao, Y., Yang, Y., Ling, W., Kong, H. & Zhu, X. Gradient distribution of root exudates and polycyclic aromatic
685 hydrocarbons in rhizosphere soil. *Soil Science Society of America Journal* **75**, 1694–1703 (2011).

686 5. Gregory, P. J. Roots, rhizosphere and soil: the route to a better understanding of soil science? *Eur J Soil Sci* **57**, 2–12 (2006).

687 6. Philippot, L., Raaijmakers, J. M., Lemanceau, P. & van der Putten, W. H. Going back to the roots: the microbial ecology of
688 the rhizosphere. *Nat Rev Microbiol* **11**, 789–799 (2013).

689 7. Kuzyakov, Y. & Blagodatskaya, E. Microbial hotspots and hot moments in soil: concept & review. *Soil Biol Biochem* **83**, 184–
690 199 (2015).

691 8. Hinsinger, P., Bengough, A. G., Vetterlein, D. & Young, I. M. Rhizosphere: biophysics, biogeochemistry and ecological
692 relevance. *Plant Soil* **321**, 117–152 (2009).

693 9. Schmidt, E. L. Initiation of plant root-microbe interactions. *Ann. Rev. Microbiol.* 355–376 (1979).

694 10. Ahmad, J. S. & Baker, R. Rhizosphere competence of *Trichoderma harzianum*. *Phytopathology* 182–189 (1987).

695 11. Weller, D. M. Biological control of soilborne plant pathogens in the rhizosphere with bacteria. *Ann. Rev. Phytopathol* **26**, 379–
696 407 (1988).

697 12. Warembourg, F. R. The ‘rhizosphere effect’: a plant strategy for plants to exploit and colonize nutrient-limited habitats.
698 *Boccone* **7**, 187–94 (1997).

699 13. Barret, M., Morrissey, J. P. & O’Gara, F. Functional genomics analysis of plant growth-promoting rhizobacterial traits
700 involved in rhizosphere competence. *Biol Fertil Soils* **47**, 729–743 (2011).

701 14. Minz, D., Ofek, M. & Hadar, Y. Plant rhizosphere microbial communities. in *The Prokaryotes* 56–84 (Springer Berlin
702 Heidelberg, Berlin, Heidelberg, 2013).

703 15. Schreiter, S. *et al.* Effect of the soil type on the microbiome in the rhizosphere of field-grown lettuce. *Front Microbiol* **5**, 144
704 (2014).

705 16. Dupuy, L. Plant-environment microscopy tracks interactions of *Bacillus subtilis* with plant roots across the entire rhizosphere.
706 *bioRxiv* (2021).

707 17. Lugtenberg, B. J. J. & Dekkers, L. C. What makes *Pseudomonas* bacteria rhizosphere competent? *Environ Microbiol* **1**, 9–13
708 (1999).

709 18. Bulgarelli, D. *et al.* Revealing structure and assembly cues for *Arabidopsis* root-inhabiting bacterial microbiota. *Nature* **488**, 91–
710 95 (2012).

711 19. Lundberg, D. S. *et al.* Defining the core *Arabidopsis thaliana* root microbiome. *Nature* **488**, 86–90 (2012).

712 20. Schlaeppi, K., Dombrowski, N., Oter, R. G., Ver Loren van Themaat, E. & Schulze-Lefert, P. Quantitative divergence of the
713 bacterial root microbiota in *Arabidopsis thaliana* relatives. *Proc Natl Acad Sci U S A* **111**, 585–92 (2014).

714 21. Tkacz, A., Cheema, J., Chandra, G., Grant, A. & Poole, P. S. Stability and succession of the rhizosphere microbiota depends
715 upon plant type and soil composition. *ISME Journal* **9**, 2349–2359 (2015).

716 22. Schneijderberg, M. *et al.* Quantitative comparison between the rhizosphere effect of *Arabidopsis thaliana* and co-occurring
717 plant species with a longer life history. *ISME J* **14**, 2433–2448 (2020).

718 23. Richter-Heitmann, T., Eickhorst, T., Knauth, S., Friedrich, M. W. & Schmidt, H. Evaluation of strategies to separate root-
719 associated microbial communities: a crucial choice in rhizobiome research. *Front Microbiol* **7**, 773 (2016).

720 24. Nemergut, D. R. *et al.* Patterns and processes of microbial community assembly. *Microbiol Mol Biol Rev* **77**, 342–56 (2013).

721 25. Sloan, W. T. *et al.* Quantifying the roles of immigration and chance in shaping prokaryote community structure. *Environ
722 Microbiol* **8**, 732–740 (2006).

723 26. Burns, A. R. *et al.* Contribution of neutral processes to the assembly of gut microbial communities in the zebrafish over host
724 development. *ISME J* **10**, 655–64 (2016).

725 27. Zhou, J. & Ning, D. Stochastic community assembly: does it matter in microbial ecology? *Microbiology and Molecular Biology
726 Reviews* **81**, (2017).

727 28. Heys, C. *et al.* Neutral processes dominate microbial community assembly in Atlantic salmon, *Salmo salar*. *Appl Environ
728 Microbiol* **86**, (2020).

729 29. Fan, K. *et al.* Rhizosphere-associated bacterial network structure and spatial distribution differ significantly from bulk soil in
730 wheat crop fields. *Soil Biol Biochem* **113**, 275–284 (2017).

731 30. Zhang, B. *et al.* Biogeography and ecological processes affecting root-associated bacterial communities in soybean fields
732 across China. *Science of the Total Environment* **627**, 20–27 (2018).

733 31. Agoussar, A. & Yergeau, E. Engineering the plant microbiota in the context of the theory of ecological communities. *Curr
734 Opin Biotechnol* **70**, 220–225 (2021).

735 32. Vieira, S. *et al.* Drivers of the composition of active rhizosphere bacterial communities in temperate grasslands. *ISME J* **14**,
736 463–475 (2019).

737 33. Normander, B. & Prosser, J. I. Bacterial origin and community composition in the barley phytosphere as a function of
738 habitat and presowing conditions. *Appl Environ Microbiol* **66**, 4372–4377 (2000).

739 34. De Ridder-Duine, A. S. *et al.* Rhizosphere bacterial community composition in natural stands of *Carex arenaria* (sand sedge) is
740 determined by bulk soil community composition. *Soil Biol Biochem* **37**, 349–357 (2005).

741 35. Berg, G. & Smalla, K. Plant species and soil type cooperatively shape the structure and function of microbial communities in
742 the rhizosphere. *FEMS Microbiol Ecol* **68**, 1–13 (2009).

743 36. Ferretti, P., Pasolli, E., Tett, A., Huttenhower, C. & Correspondence, N. S. Mother-to-infant microbial transmission from
744 different body sites shapes the developing infant gut microbiome. *Cell Host Microbe* **24**, 133–145 (2018).

745 37. López, J. L. *et al.* Growth rate is a dominant factor predicting the rhizosphere effect. *ISME J* **17**, 1396–1405 (2023).

746 38. Dini-Andreote, F. & Raaijmakers, J. M. Embracing community ecology in plant microbiome research. *Trends Plant Sci* **23**,
747 467–469 (2018).

748 39. Stringlis, I. A. *et al.* MYB72-dependent coumarin exudation shapes root microbiome assembly to promote plant health.
749 *PNAS* (2018).

750 40. Hill, M. O. Diversity and evenness: a unifying notation and its consequences. *Ecology* **54**, 427–432 (1973).

751 41. Cao, Q. *et al.* Effects of rare microbiome taxa filtering on statistical analysis. *Front Microbiol* **11**, 3203 (2021).

752 42. Parras-Moltó, M. & Cácer, D. A. de. Assessment of phylo-functional coherence along the bacterial phylogeny and
753 taxonomy. *Scientific Reports* **2021** *11*:1 **11**, 1–6 (2021).

754 43. Faith, D. P. Conservation evaluation and phylogenetic diversity. *Biol Conserv* **61**, 1–10 (1992).

755 44. Vellend, M. *The Theory of Ecological Communities*. (Princeton University Press, New Jersey, USA, 2016).

756 45. Wennekes, P. L., Rosindell, J. & Etienne, R. S. The neutral-niche debate: a philosophical perspective. *Acta Biotheor* **60**, 257–71
757 (2012).

758 46. Leibold, M. A. & McPeek, M. A. Coexistence of the niche and neutral perspectives in community ecology. *Ecology* **87**, 1399–
759 1410 (2006).

760 47. Hubbel, S. P. *A Unified Theory of Biodiversity and Biogeography*. (Princeton University Press, New Jersey, USA, 2001).

761 48. Chase, J. M. & Myers, J. A. Disentangling the importance of ecological niches from stochastic processes across scales. *Philos
762 Trans R Soc Lond B Biol Sci* **366**, 2351–63 (2011).

763 49. Langenheder, S. & Székely, A. J. Species sorting and neutral processes are both important during the initial assembly of
764 bacterial communities. *ISME J* **5**, 1086–1094 (2011).

765 50. Mendes, R. *et al.* Deciphering the rhizosphere microbiome for disease-suppressive bacteria. *Science* (1979) **322**, 1097–1100
766 (2011).

767 51. Sessitsch, A. *et al.* Functional characteristics of an endophyte community colonizing rice roots as revealed by metagenomic
768 analysis. *Molecular Plant-Microbe Interactions* **25**, 28–36 (2012).

769 52. Thiergart, T. *et al.* Root microbiota assembly and adaptive differentiation among European *Arabidopsis* populations. *Nat Ecol
770 Evol* **4**, 122–131 (2020).

771 53. Zamioudis, C., Mastranesti, P., Dhonukshe, P., Blilou, I. & Pieterse, C. M. J. Unraveling root developmental programs
772 initiated by beneficial *Pseudomonas* spp. bacteria. *Plant Physiol* **162**, 304–18 (2013).

773 54. Berendsen, R. L. *et al.* Unearthing the genomes of plant-beneficial *Pseudomonas* model strains WCS358, WCS374 and
774 WCS417. *BMC Genomics* **16**, 539 (2015).

775 55. Pieterse, C. M. J. *et al.* *Pseudomonas simiae* WCS417: star track of a model beneficial rhizobacterium. *Plant and Soil* **2020** *461*:1
776 **461**, 245–263 (2020).

777 56. Fierer, N., Bradford, M. A. & Jackson, R. B. Toward an ecological classification of soil bacteria. *Ecology* **88**, 1354–1364
778 (2007).

779 57. von Meijenfeldt, F. A. B., Hogeweg, P. & Dutilh, B. E. A social niche breadth score reveals niche range strategies of
780 generalists and specialists. *Nature Ecology & Evolution* **2023** *7*:7, 768–781 (2023).

781 58. Song, H. K. *et al.* Bacterial strategies along nutrient and time gradients, revealed by metagenomic analysis of laboratory
782 microcosms. *FEMS Microbiol Ecol* **93**, (2017).

783 59. Bulgarelli, D., Schlaeppi, K., Spaepen, S., van Themaat, E. V. L. & Schulze-Lefert, P. Structure and functions of the bacterial
784 microbiota of plants. *Annu Rev Plant Biol* **64**, 807–838 (2013).

785 60. Lebeis, S. L. *et al.* Salicylic acid modulates colonization of the root microbiome by specific bacterial taxa. *Science* (1979) **349**,
786 860–864 (2015).

787 61. Wippel, K. *et al.* Host preference and invasiveness of commensal bacteria in the *Lotus* and *Arabidopsis* root microbiota. *Nature
788 Microbiology* **2021** *6*:9 **6**, 1150–1162 (2021).

789 62. Bodenhausen, N., Horton, M. W. & Bergelson, J. Bacterial communities associated with the leaves and the roots of
790 *Arabidopsis thaliana*. *PLoS One* **8**, e56329 (2013).

791 63. Peiffer, J. A. *et al.* Diversity and heritability of the maize rhizosphere microbiome under field conditions. *Proc Natl Acad Sci U
792 S A* **110**, 6548–53 (2013).

793 64. Niu, B., Paulson, J. N., Zheng, X. & Kolter, R. Simplified and representative bacterial community of maize roots. *Proc Natl
794 Acad Sci U S A* **114**, E2450–E2459 (2017).

795 65. Turner, T. R. *et al.* Comparative metatranscriptomics reveals kingdom level changes in the rhizosphere microbiome of plants.
796 *ISME Journal* **7**, 2248–2258 (2013).

797 66. Ofek, M., Voronov-Goldman, M., Hadar, Y. & Minz, D. Host signature effect on plant root-associated microbiomes
798 revealed through analyses of resident vs. active communities. *Environ Microbiol* **16**, 2157–2167 (2014).

799 67. Schlatter, D. C., Yin, C., Hulbert, S. & Paulitz, T. C. Core rhizosphere microbiomes of dryland wheat are influenced by
800 location and land use history. *Applied Environmental Microbiology* **86**, (2020).

801 68. Ofek, M., Hadar, Y. & Minz, D. Ecology of root colonizing *Massilia* (Oxalobacteraceae). *PLoS One* **7**, e40117 (2012).
802 69. Yu, P. *et al.* Plant flavones enrich rhizosphere Oxalobacteraceae to improve maize performance under nitrogen deprivation.
803 *Nat Plants* 1–19 (2021) doi:10.1038/s41477-021-00897-y.
804 70. Vismans, G. *et al.* Coumarin biosynthesis genes are required after foliar pathogen infection for the creation of a microbial
805 soil-borne legacy that primes plants for SA-dependent defenses. *Scientific Reports* **2022 12:1** 12, 1–12 (2022).
806 71. Mendes, L. W., Kuramae, E. E., Navarrete, A. A., van Veen, J. A. & Tsai, S. M. Taxonomical and functional microbial
807 community selection in soybean rhizosphere. *ISME J* **8**, 1577–1587 (2014).
808 72. Munoz-Ucros, J., Zwetsloot, M. J., Cuellar-Gempeler, C. & Bauerle, T. L. Spatiotemporal patterns of rhizosphere
809 microbiome assembly: from ecological theory to agricultural application. *Journal of Applied Ecology* vol. 58 894–904 (2021).
810 73. Berendsen, R. L. *et al.* Disease-induced assemblage of a plant-beneficial bacterial consortium. *ISME J* **12**, 1496–1507 (2018).
811 74. Murashige, T. & Skoog, F. A revised medium for rapid growth and bio assays with tobacco tissue cultures. *Physiol Plant* **15**,
812 473–497 (1962).
813 75. Caporaso, J. G. *et al.* QIIME allows analysis of high-throughput community sequencing data. *Nature Methods* **2010 7:5** 7, 335–
814 336 (2010).
815 76. Martin, M. Cutadapt removes adapter sequences from high-throughput sequencing reads. *EMBnet J* **17**, 10–12 (2011).
816 77. Callahan, B. J. *et al.* DADA2: High-resolution sample inference from Illumina amplicon data. *Nat Methods* **13**, 581–583
817 (2016).
818 78. Rognes, T., Flouri, T., Nichols, B., Quince, C. & Mahé, F. VSEARCH: A versatile open source tool for metagenomics. *PeerJ*
819 **2016**, e2584 (2016).
820 79. Bokulich, N. A. *et al.* Optimizing taxonomic classification of marker-gene amplicon sequences with QIIME 2's q2-feature-
821 classifier plugin. *Microbiome* **6**, 1–17 (2018).
822 80. McMurdie, P. J. & Holmes, S. Phyloseq: an R package for reproducible interactive analysis and graphics of microbiome
823 census data. *PLoS One* **8**, e61217 (2013).
824 81. Weissman, J. L., Hou, S. & Fuhrman, J. A. Estimating maximal microbial growth rates from cultures, metagenomes, and
825 single cells via codon usage patterns. *Proceedings of the National Academy of Sciences* **118**, e2016810118 (2021).
826